Biogeochemistry **39:** 343–375, 1997.

Soil organic carbon dynamics: variability with depth in forested and deforested soils under pasture in Costa Rica

DOUWE VAN DAM[1], EDZO VELDKAMP[2] & NICO VAN BREEMEN[1]
[1]*Department of Soil Science and Geology, Wageningen Agricultural University, P. O. Box 37, 6700 AA Wageningen, The Netherlands;* [2]*Institut für Bodenkunde und Waldernährung, Georg-August Universität Göttingen, 37077 Göttingen, Germany*

Accepted 6 June 1997

Key words: ^{13}C, ^{14}C, land use change, model, soil organic carbon, tropical forest

Abstract. Dynamics of soil organic carbon (SOC) in chronosequences of soils below forests that had been replaced by grazed pastures 3–25 years ago, were investigated for two contrasting soil types (Andic Humitropept and Eutric Hapludand) in the Atlantic Zone of Costa Rica. By forest clearing and subsequent establishment of pastures, photosynthesis changes from a C-3 to a C-4 pathway. The accompanying changes in C-input and its δ^{13}C and ^{14}C signals, were used to quantify SOC dynamics. C-input from root turnover at a pasture site was measured by sequential harvesting and ^{14}C-pulse labelling. With a spatial resolution of 5 cm, data on total SOC, δ^{13}C and δ^{14}C of soil profiles were interpreted with a model that distinguishes three pools of SOC: 'active' C, 'slow' C and 'passive' C, each with a $1^{-\text{st}}$ order decomposition rate (k_a, k_s and k_p). The model includes carbon isotope fractionation and depth-dependent decomposition rates. Transport of C between soil layers was described as a diffusion process, which accounts for physical and biotic mixing processes.

Calibrated diffusion coefficients were 0.42 cm^2 yr^{-1} for the Humitropept and 3.97 cm^2 yr^{-1} for the Hapludand chronosequence. Diffusional transport alone was insufficient for optimal simulation; it had to be augmented by depth-dependent decomposition rates to explain the dynamics of SOC, δ^{13}C and δ^{14}C. Decomposition rates decreased strongly with depth. Upon increased diffusion, differences between calibrated decomposition rates of SOC fractions between surface soils and subsoils diminished, but the concept of depth-dependent decomposition had to be retained, to obtain small residuals between observed and simulated data. At a reference depth of 15–20 cm k_s was 90 yr^{-1} in the Humitropept and 146 yr^{-1} in the Hapludand. Slow C contributed most to total organic C in surface soils, whereas passive C contributed most below 40 cm depth. After 18–25 years of pasture, net loss of C was 2180 g C m^{-2} for the Hapludand and 150 g m^{-2} for the Humitropept soil.

Introduction

Soil organic matter (SOM) has important functions in natural and agro-ecosystems. It (1) helps to build and stabilize soil structure relevant for aeration and water supply, (2) buffers supply of plant nutrients, and (3) plays a major role in the global biogeochemical budgets of the greenhouse gases CO_2, CH_4 and N_2O and other biotic trace gases (Bouwman 1990; Keller et al. 1993). Deforestation generally leads to decreased contents of soil organic carbon (SOC), with associated loss of soil fertility and increased emission of greenhouse gases. Increasing soil carbon stock after forest clearing to pasture has been reported too (Lugo & Brown, 1993; Fisher et al. 1994), especially for well managed pastures. Yet, the net release of C from the world's tropics due to deforestation in the 1980's was about 1.60 Pg C yr^{-1} (Schimel 1995), of which 0.1–0.3 Pg C yr^{-1} came from decomposition of SOM (Detwiler & Hall 1988). This carbon release from tropical areas is second only to the global release from fossil fuel burning (5.4 Pg C yr^{-1}, Sundquist 1993). Loss of soil organic carbon is less after deforestation to pastures than to cropland (Detwiler 1986), but pastures play a key role due to the large area they cover (Houghton et al. 1991).

In the Atlantic Zone of Costa Rica large areas of tropical lowland forest have been cleared in the last 40 years (Veldkamp et al. 1992), mostly to pasture (Huising 1993). Deforestation to low-productive pastures resulted in a net loss of between 150 and 2180 g C m^{-2} over 25 years, depending on the soil type (Veldkamp 1994).

SOC contents are the result of input of plant debris, decomposition, and transport of C between soil layers. These processes are often integrated by dynamic simulation modelling. Most models consider only one soil compartment with 2–5 SOC pools, characterized by different first-order decay rates, which are sometimes constrained by considering ^{14}C dynamics (Jenkinson 1990; Parton et al. 1988, 1993; Rastetter et al. 1991). Such models ignore a number of aspects typical of soil profiles: (1) SOC contents in non-arable soils normally strongly decrease with increasing soil depth, (2) SOC decomposition rates commonly decrease with depth, and (3) vertical transport of SOC by mixing and leaching is common in many soils. These processes may need to be considered to explain the steep increase in ^{14}C age of SOC with depth in most soils (Scharpenseel et al. 1989). For forest soils in Eastern Amazonia Trumbore et al. (1995) concluded that passive C increased from 5–10% at 0–10 cm depth to 90% below 3 m depth, and that its turnover rate decreased strongly with depth, as evinced by strongly decreasing Δ^{14}C values. Hunt (1977) invoked decreasing decomposition rates with depth in SOC dynamics, because his model suggested that temperature and moisture could not account for the large differences in SOC dynamics at different depth. He suspected that the decreasing decomposition rates were related to decreasing oxygen concentration with depth. Detwiler (1986) concluded that after clearing of tropical forests and conversion to pastures, SOC contents usually decrease much more rapidly in surface soils than in deeper soil horizons. Skjemstad et al. (1990) attributed slower decomposition of SOC at greater soil depth in subtropical rainforest to protection of soil C in microaggregates. In addition to vertical transport of SOC, Nakane (1978a, 1978b) had to assume decreasing decomposition rates with depth to explain SOC profiles in forest soils. Elzein and Balesdent (1995), on the other hand, concluded that vertical transport of C alone could explain SOC profiles and age of SOC with depth.

The aim of this paper is to test the importance of such depth-dependent processes. We used a simple SOC dynamics model that describes the dynamics of ^{13}C and ^{14}C at various depths in soil profiles in addition to that of ^{12}C. The model is calibrated for forest-pasture chronosequences on two contrasting soil types in Costa Rica, in which the change of C-3 (forest) to C-4 (pasture) vegetation gives rise to increased δ^{13}C in carbon input (Balesdent et al. 1988).

Material and methods

Study sites

The study was carried out in the Atlantic Zone of Costa Rica. The climate is humid tropical; mean annual temperature is 26 °C and mean annual precipitation is 3000–6000 mm, with precipitation exceeding evapotranspiration in each month. The studied soils are at ± 100 m altitude on the foot slopes of the Turrialba volcano, formed in andesitic laharic, fluvio-laharic and fluvial deposits. Tropical lowland rain forest is the natural vegetation. Forest-pasture chronosequences were selected for two soil types, a Holocene, sandy, fertile, Eutric Hapludand (forest and 25 yr pasture after deforestation), and a Pleistocene, deeply weathered, clayey, nutrient-poor Andic Humitropept (forest and 3, 5, 10 and 18 yr low-productive pasture after deforestation). The dominant native grass species in the pastures is *Axonopus compressus*. Some selected soil characteristics are presented in Table 1. The soils at all sampling sites are level, without any sign of erosion.

Primary production

Primary production of the forest sites and pools and turnover rates of C in tree compartments were taken from Raich (1980, 1983) for similar soils in the Atlantic zone of Costa Rica (Table 2). Aboveground production of low yielding *Axonopus compressus*, dominant in native pasture, on a Hapludand was reported as 580 g C $m^{-2}yr^{-1}$ (CATIE 1989).

We determined above- and belowground production of *Axonopus compressus* as follows. Young plants from stolons collected in actively grazed pastures were grown in 30 PVC tubes of 0.159 m ID and 0.5 m length. The tubes were inserted in the 25 yr pasture Hapludand, 0.7 m apart. The area between the tubes was kept free of vegetation. After three months, the plants completely covered the columns and were cut at 0.05 m above the soil surface. Cutting was repeated every 4 weeks, to mimic effects of grazing on

Table 1. Selected characteristics of Hapludand and Humitropept soils under forest and pasture

	depth cm	sand %	silt %	clay %	pH H_2O	CEC cmol kg^{-1}	base saturation %
Eutric Hapludand							
forest	0–25	59	28	13	5.3	21.0	43
	25–80	68	27	5	5.6	5.9	15
	80–90	77	20	3	5.7	5.4	35
pasture (25yr)	0–7	62	36	2	4.2	17.1	53
	7–20	63	36	0	5.5	16.2	37
	20–70	71	29	0	5.8	9.0	47
	70–100	80	17	3	6.0	5.5	45
Andic Humitropept							
forest	0–15	6	24	69	3.9	19.4	6
	15–60	7	29	64	4.3	10.0	1
	60–140	6	26	68	4.4	9.2	1
pasture (18yr)	0–23	9	37	54	4.5	18.3	39
	23–110	9	29	62	4.6	13.9	23
	110–140	8	27	66	4.6	8.2	2

above- and belowground production. After another four months, 13 subsequent four-week's cuttings (3 replicates) were used to determine aboveground production throughout the year. Belowground production was determined by pulse labelling with $^{14}CO_2$ on five occasions throughout the year (3 replicate tubes), at times representative for both wet and drier seasons. Plants were pulse labelled with $^{14}CO_2$ two weeks before the next cutting. We labelled during sunny mornings when plants were photosynthesizing actively. After covering them with transparent plastic bags sealed to the PVC tubes, the plants received 1.95 MBq of $^{14}CO_2$, released by addition of excess HCl to a vial containing dissolved $Na_2{}^{14}CO_3$. Label remaining in the vial was transferred to the bag by injecting extra air through the vial into the bag. Two hours later, unlabelled CO_2 was added in the same way, to maintain photosynthetic activity of the plants. Plastic bags were removed 4 h after labelling commenced, and plants were then allowed to grow normally in the open air. Two weeks after label application, shoots were cut flush with the soil surface, and the PVC tubes were dug out. The soil columns were cut into samples from 0–1, 1–5, 5–10, 10–15, 15–20, 20–30, 30–40 and 40–50 cm depth. Each sample was crushed manually and the roots were separated from the soil by hand picking. Dry weights of shoots, roots and soil were determined after drying at 75 °C for 24 h. The root and shoot material was milled (< 1 mm). Total C and ^{14}C of plant material and soil were determined by titration and scintillation counting after conversion to CO_2 by wet-combustion according to Amato (1983). The ratio between measured ^{14}C activity of above- and belowground plant parts two weeks after label application was assumed to represent the ratio between above- and belowground production during the two weeks after label application. A significant linear relation ($r^2 = 0.58$) between aboveground dry matter production and the ratio between above- and belowground production for all individually labelled plants was combined with the 13 four-weeks' above-ground harvests to calculate the belowground production throughout the year.

Bulk density, SOC, $\delta^{13}C$ and $\delta^{14}C$

To compare amounts of SOC in forest and pasture sites on a common weight basis, dry bulk density of soil was determined at 10 depths, using 300 cm^3 stainless steel rings ($n \geq 8$). The samples were oven-dried for 24 h at 105 °C. Total soil organic carbon, ^{13}C and ^{14}C were determined at the Centre for Isotope Research of the University of Groningen for composite samples of the replicates of the bulk density determinations from which roots had been removed by hand picking. Prior to ^{13}C determination soil samples were ground and treated with 1N HCl to remove any $CaCO_3$, and then oven dried at 80 °C. About 1 g of the samples was burned in the presence of Cu-oxide under pure O_2 at 900 °C. Water vapour was trapped on dry ice. CO_2 and NO_x were trapped in liquid air (–186 °C). O_2 was evacuated and NO_x was reduced to N_2 in the presence of Cu. The remaining pure CO_2 was trapped with help of liquid N_2, and its pressure at constant volume and temperature was used to calculate the C content of the samples. ^{13}C was analyzed with a SIRA 9 mass spectrometer. The laboratory reference was calibrated against Pee-Dee Belemnite, using the international standard NBS 19. Analytical precision expressed as the standard deviation obtained on different combustions of the same homogenized sample was better than 0.05‰ $\delta^{13}C$. The δ notation (in units of ‰) as employed here is defined as $\delta X = ((R_{sa}/R_{st}) - 1) \times 1000$, where R is the isotope ratio (atom %) of a sample (sa) and a standard (st). ^{14}C activities were determined by conventional counting of desintegrations from pure benzene synthesized from CO_2 obtained from the bulk soil samples (Mook & Streurman 1983). $\delta^{14}C$ values are expressed relative to 0.95 of the ^{14}C activity of the NBS oxalic acid standard. Radiocarbon measurements intended for age determinations are usually standardized against pre-1900 wood with a $\delta^{13}C$ value of –25‰ to account for isotope fractionation effects of ^{12}C against ^{13}C and ^{14}C. In our study $\delta^{14}C$ data were intentionally *not* corrected for isotopic fractionation, because isotopic fractionation against ^{13}C and ^{14}C is accounted for in our model.

Soil respiration

To test the effect of soil depth on decomposition rates, soil samples (4 g air-dry weight) of the Hapludand (forest and 25 yr pasture) and the Humitropept (forest and 18 yr pasture) from eight 5-cm layers selected from between 0 and 50 cm depth were incubated in closed vessels at 20 °C and a moisture content of 100% (w/w). CO_2 production was monitored hourly for 5 weeks by measuring the decrease of electrical conductivity of a 0.1 m KOH solution upon adsorption of CO_2 (Nordgren 1988). The first week was considered to be a pre-incubation, and the CO_2 evolution during the next four weeks is reported here. To study whether the observed differences in soil respiration between depths were caused by differences in supply of nutrients or of easily decomposable substrate, we also measured CO_2 production in Hapludand forest surface soil (0–5 cm) and subsoil (55–60 cm) samples after adding: (i) demineralized water, (ii) nutrient solution, (iii) glucose (1365 mg/l of glucose-C), and (iv) glucose + nutrient solution. The full strength nutrient solution contained (concentrations in mmol/l between parentheses): NH_4NO_3 (1), $MgSO_4.7H_2O$ (0.27), KCl (0.98), K_2HPO_4 (0.19), $CaCl_2.2H_2O$ (0.41), H_3BO_3 (0.02), Fe (0.04), and trace quantities (μmol/l) of Mn (2), Zn (0.85), Mo (0.25), and Cu (0.15). Two weeks later the addition of glucose was repeated, but then without nutrients and dissolved in 1 ml only of demineralized water. The other treatments received also 1 ml of demineralized water, to maintain the same moisture content in all treatments. Respiration of glucose was calculated from the difference between CO_2 production of the treatments with and without glucose addition.

Model description

SOC dynamics and cycling of carbon isotopes is described with a basically simple model with three soil organic carbon (SOC) pools that decay according to 1st-order kinetics (Figure 1). Input of plant debris (I) enters a 'active' SOC pool (C_a), which is decomposed at rate k_a, partly ($1-\varepsilon_a$) to CO_2, and partly (ε_a) to a 'slow' SOC pool (C_s). Similarly, C_s is decomposed at rate k_s, partly to CO_2 ($1-\varepsilon_s$), the remaining part being transferred to 'passive' SOC, C_p. Finally, C_p is respired to CO_2 at rate k_p. Such kind of dynamics is common in many SOC models, such as CENTURY (Parton et al. 1988, 1992), the Rothamsted model (Jenkinson 1990) and SOCRATES (Grace & Lad 1995).

Details of our model are as follows:

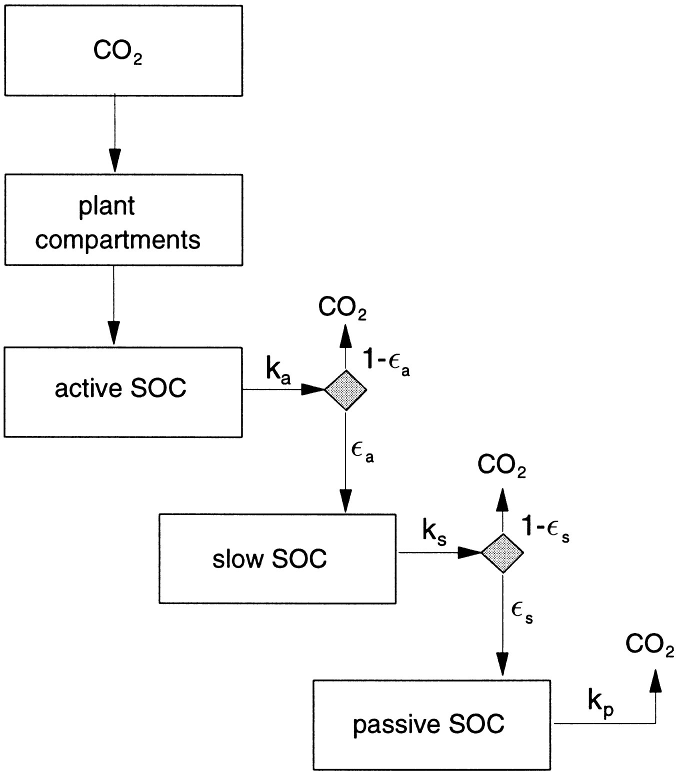

Figure 1. General structure of the soil organic carbon model used in this study. Parameters k_a, k_s and k_p are first order rate constants, and ϵ_a and ϵ_s are dimensionless coefficients regulating the partitioning of C between respiration and stabilization into a next older pool.

a) Plant debris is separated into material derived from leaves, branches, stems, fine roots (< 2 mm), medium roots (2–10 mm), and coarse roots (> 10 mm). Each of those plant compartments has a specific 1st-order turnover rate. The contribution to total root biomass of different diameter classes of forest roots, each with their own specific residence time, gives rise to plant debris input of different age at different depth in the soil profile. After deforestation, remaining dead tree roots continue to contribute to SOC input. For pasture roots no diameter classes were distinguished; their turnover rates varied with depth as determined by the ^{14}C-pulse labelling experiment. For the pasture sites it was estimated that by grazing 20% of C in aboveground primary production was lost to the atmosphere as CO_2. This estimate is based on a measured liveweight gain of cattle of 158 kg ha^{-1} yr^{-1} at a stocking rate of 1.7 animal ha^{-1} (Ibrahim 1994) and tables for calculating forage intake from growth of beef cattle (Minson & McDonald) at 350 kg live weight and a dry matter digestibilty of 55%.

b) ^{12}C, ^{13}C and ^{14}C are distinguished for each compartment, as well as for atmospheric input signals. We assumed that forest leaves had slightly less ^{13}C (δ^{13}C = –31.5‰) than the rest of the tree (δ^{13}C = –30.75‰), cf. Vittorello et al. (1989) and Skjemstad et al. (1990). Above-ground pasture C had a δ^{13}C value of –15‰, for the pasture roots a δ^{13}C value of –14.75:‰ was used. The decrease in atmospheric δ^{13}C due to burning of fossil fuel, the so-called ^{13}C Suess effect, is accounted for by an exponential function, which we derived by fitting tree ring data given by Leavit and Long (1988):

$$\Delta\delta^{13}\mathrm{C} = -3.7((\mathrm{T} - 1450) \times 0.0015)^3 \qquad (-50 < \mathrm{T} < 1450)$$

with $\Delta\delta^{13}$C being the change in δ^{13}C in plant compartments since 1450 B.P., and T the time in years B.P.. Northern hemisphere ^{14}C activity of atmospheric CO_2 was taken from Nydal and Lovseth (1983), and exponentially extrapolated for years after 1975, to fit observed values during summer months near Groningen, the Netherlands (cf. Figure 1 and Appendix 1 in Meyer & van der Plicht 1995). Pre-bomb variations in ^{14}C activity were ignored.

^{13}C/^{12}C ratios change during decomposition of plant material in soil, mainly due to kinetic isotope fractionation during microbial respiration of SOC (Stout et al. 1981; Blair et al. 1985; Bertram, 1986; Nadelhofffer & Fry 1988). We assumed that respiration rates for ^{13}C are slower than those for ^{12}C by an isotope discrimination factor α, *i.e.* $k_h = k_l (1 - \alpha)$, with k_l representing the respiration rate for the light isotope (^{12}C) and k_h the rate for the heavy isotope (^{13}C). Furthermore we assumed that with respect to ^{12}C isotope discrimination was twice as high for ^{14}C than for ^{13}C.

c) We described transport of SOC between soil layers by physical and biotic mixing processes as an analogy of a diffusion process according to:

$$\partial C/\partial t = D\partial^2 C/\partial z^2 \qquad (1)$$

where ∂C/∂t (kg cm^{-2} yr^{-1}) is the rate of transport per surface area, between soil layers for which the distance between nodes is z. The diffusion coefficient D has units of cm^2 yr^{-1}, if the concentration of C is expressed in g cm^{-3}, t is in years and z in cm. Convective transport of C, e.g. of dissolved C, is not explicitly accounted for in our model, but may occur and be partly represented parametrically by the fitted diffusion constant D. Except for podzolic soils, convective transport seems to be unimportant relative to diffusional transport (Elzein & Balesdent 1995).

d) Depth-dependent decomposition
In our model, depth discretization dz is into 5 cm layers, and decomposition rates of SOC fractions (C_a, C_s and C_p) vary with depth, according to a so-called biological switch function (cf. Thornley and Johnson 1990, p. 147):

$$r_z = p_1 + (p_2 - p_1) \cdot z^{p3}/(z^{p3} + p_4{}^{p3}) \tag{2}$$

in which r_z is the relative decomposition rate at depth z and p_1, p_2, p_3 and p_4 are fitting parameters, which differed for forest and pasture sites. We standardized r_z for the 15–20 cm layer of the forest soils to a value of 1, so that three parameters (p_1/p_2, p_3 and p_4; $p_1 = 1$) suffice to describe this function for the forest sites. Calibrated r_z functions for forest and pasture sites are visualized in Figure 6.

e) Numerical implementation and discretization
Without any transport of C the model can be solved analytically. Each carbon pool at time t (Q_t) is calculated from its size at the end of a previous timestep (Q_0) according to:

$$Q_t = Q_0 + I - O \tag{3}$$

where I is the input and O is the output during a time increment dt. The output is calculated as

$$O = Q_0(1 - e^{-k.dt}) + \mathbf{I}(1 - (1 - e^{-k.dt})(k \cdot dt)^{-1}) \tag{4}$$

where k is the first order reaction rate for ^{12}C + ^{13}C (TOC). Equation (4) is valid in any condition and values of dt, provided that the input during a time increment dt remains constant. The second part of equation (4) equals the integral over time of output originating from input during a time increment dt.

An example demonstrates that k for TOC is negligibly affected by isotope discrimination against ^{13}C, and therefore it can be equated to the reaction rate constant for ^{12}C: let α be as high as 0.005, ϵ as low as 0.25, and let the isotope ratio ^{13}C/TOC be as high as 0.012 ($\delta^{13}C$ = 68), then for infinitely small dt

$$d^{12}C/dt = TOC \cdot 0.988 \cdot k_{12C} \tag{5a}$$

$$d^{13}C/dt = TOC \cdot 0.012 \cdot k_{12C} \cdot 0.75 \cdot (1 - 0.005) + TOC \cdot 0.012 \cdot k_{12C} \cdot 0.25 \tag{5b}$$

$$dTOC/dt = TOC \cdot 0.999955 \cdot k_{12C} = TOC \cdot k \approx TOC \cdot k_{12C} \tag{5c}$$

Including the effects of depth-dependent decomposition (r_z of Equation (2), isotope discrimination during respiration (α), and radioactive decay, the rate constants used for ^{12}C, ^{13}C and ^{14}C are:

$$k_{12C} = k \cdot r_z \cdot ((1-\epsilon) + \epsilon) \tag{6a}$$

$$k_{13C} = k \cdot r_z \cdot ((1-\epsilon) \cdot (1-\alpha) + \epsilon) \tag{6b}$$

$$k_{14C} = k \cdot r_z \cdot ((1-\epsilon) \cdot (1-2\alpha) + \epsilon) + k_L \tag{6c}$$

Equations 6a–c indicate that isotope discrimination against the heavier isotopes is assumed to occur in the respiration step only, and not in the process of transfer into a more stable pool. The radio-active decay rate constant (k_L) is obtained from the half-life (5730 yr) of ^{14}C

$$k_L = \ln(2)/5730 \tag{7}$$

Output of ^{14}C due to radio-active decay (O_{rad}) is calculated as

$$O_{rad} = O \cdot k_L/(k_L + k_{14C}) \tag{8}$$

The non-radio-active part of the output ($O - O_{rad}$) is partly due to respiration (O_r) and for the rest due to transfer (humification) into a next pool (O_h), for which it serves as input.

$$O_r = (O - O_{rad}) \cdot (1-\epsilon) \tag{9}$$

$$O_h = (O - O_{rad}) \cdot \epsilon \tag{10}$$

An advantage of analytical solutions is that state variables can be calculated for large time steps. However, analytical solutions are not possible for non-steady state conditions if diffusional transport is introduced into the model. A numerical approximation can be obtained by simply adding transport fluxes between adjacent soil layers to the no-transport analytical model, using sufficiently small time increments. State variables for steady state forest situations were calculated by initializing t at 27000 yr BP, proceeding with dt's of 10 yr until 7000 yr BP, dt's of 2 yr between 7000 yr and 2000 yr BP, and by using dt's of 1 yr after 2000 yr BP. Diffusional transport between adjacent soil layers was calculated with dt's that were 8 times smaller than dt's used in calculating the other fluxes. At high values of the diffusion coefficient D, numerical dispersion during the initial millennia was unacceptably high. However, after 1000BP state variables appeared to differ by less than 0.1% if dt's were decreased any further if $D \leq 8$ cm^2 yr^{-1}. Spatial discretization dz was 5 cm, in line with the sampling depths, and any numerical dispersion due to this depth discretization was ignored.

Model calibration and sensitivity analysis

To explore the relative importance of diffusional transport and depth-dependent decomposition rates, the model was first calibrated for fixed decomposition rates with depth and variable diffusion coefficients D. Next calibration was done for different fixed values of the diffusion coefficient D and concurrent variable decomposition rates with depth. We used non-linear inverse modelling to calculate optimum values for model parameters, by minimizing the sum of squared residuals between observed and simulated values of SOC, ^{13}C and ^{14}C. Residuals were minimized with a Simplex algorithm (Caceci & Cacheris 1984; Nelder & Mead 1965). To simulate SOC contents at various depths with the same relative accuracy, amounts of SOC were first log-transformed. The Humitropept and Hapludand chronosequences were each considered as one data set, for which the overall sum of residuals of log(SOC), $\delta^{13}C$ and $\delta^{14}C$ should be minimized. This necessitated the introduction of some arbitrary weighing factors for these residuals. Although $\delta^{14}C$ was determined for fewer depth intervals than SOC and $\delta^{13}C$, we decided that for the Hapludand site log(SOC), $\delta^{13}C$ and $\delta^{14}C$ should be simulated with about equal residuals. The same weighing factors were used for the Hapludand and Humitropept chronosequences.

After calibration, the parameters were varied simultaneously, using a uniform distribution of –2.5 to +2.5% around their optimum values. The RSS of 2000 such runs for both chronosequences were then used to calculate parameter sensitivities, expressed as their Kolmogorov-Smirnov d-value, which is the maximum of the absolute difference between cumulative distributions of accepted and rejected runs. Simulations were accepted if residuals for SOC, $\delta^{13}C$ and $\delta^{14}C$ were all three below their minimum + 2 times their standard deviation. Because our data on SOC and its isotopic composition were not replicated, we could not calculate probability limits of parameters.

Results

Primary production and C-input to the soil

Aboveground production in the tubes was 54% higher than in a field experiment for the same grass species at the same soil (CATIE 1989). Therefore, to obtain realistic dry matter production estimates our aboveground production data were multiplied by 0.65, and we combined this estimate with a regression equation between aboveground production and C-allocation to roots for all individually labelled tubes ($r^2 = 0.58$) to calculate the belowground production in the field. Investment in roots vs. shoots increased upon declining shoot production. Aboveground production in the tubes was significantly lower in the dry season (32 g C m^{-2} $month^{-1}$) than in the wet season (44 g C m^{-2} $month^{-1}$).

In the dry season a higher proportion of the root growth was in deeper layers, than in the wet season, when $>$ 75% of the root growth was in the top

Table 2. Pool sizes, carbon allocation and turnover rates of tree compartments for native tropical forest at the Humitropept and Hapludand sites (after Raich 1980, 1983). Carbon allocation to tree compartments and their turnover rates are model parameters to match poolsizes, and a NPP which was 850 g C m^{-2} yr^{-1} at the Humitropept and 1400 g C m^{-2} yr^{-1} at the Hapludand soil

	pool size (g C m^{-2})		allocation (% of NPP)		turnover
	Humitropept	Hapludand	Humitropept	Hapludand	rate (yr^{-1})
leaves	580	1020	38.0	41.0	0.56
branches	2720	4200	16.0	15.0	0.05
stems	15300	23800	18.0	17.0	0.01
coarse roots	450	680	0.5	0.5	0.01
medium roots	300	450	4.0	3.5	0.11
fine roots	200	320	23.5	23.0	1.00

5 cm (Table 3). Calculated below-ground production varied from 31 g C m^{-2} $month^{-1}$ in the dry season to 24 g C m^{-2} $month^{-1}$ in the wet season. Annual root growth at different depths was estimated by adding up the monthly root growth numbers. The residence time (RT) of carbon in the grass roots is based on the calculated growth with depth and the distribution of root biomass in the 25 yr old pasture at the Hapludand soil (Table 4). Biomass and production of roots was concentrated in the upper 5 cm, and residence time of roots decreased from about 1 year in the upper 10 cm to more than 3 year below 50 cm depth.

Aboveground dry matter production on the Humitropept was determined to be 500 g C m^{-2} yr^{-1} (M. Ibrahim, pers. comm.) and we assumed a similar ratio of root/shoot production as on the Hapludand. Root biomass with depth was measured on both soil types and we assumed equal distribution of root growth with depth for the Humitropept and the Hapludand.

Bulk density, carbon stocks, and isotope characteristics of soil profiles

Bulk density increased with pasture age (Table 5), with most of the compaction occurring immediately after forest clearing. Soil organic carbon (SOC) and δ^{13}C values (Table 6) were measured on samples taken in 1992 and discussed by Veldkamp (1994). Forest and the oldest pasture sites were resampled in 1994 at four different depths for bulk δ^{14}C analysis (Table 6). For both soils, δ^{14}C numbers decreased with depth. This decrease was stronger for the Humitropept (around –285 at 55 cm depth) than for the Hapludand (around –80 at 55 cm depth). In all cases the pasture values were lower than the forest values, with the exception of the Hapludand at 25 cm depth. In the forest soils δ^{13}C increased with depth, as has been frequently observed in many other

Table 3. Distribution of ^{14}C activity two weeks after pulse labelling in roots of *Axonopus compressus* at different depth during wet and dry seasons at the Hapludand site. The distribution of ^{14}C with depth in roots is given as % of total recovery in roots with standard deviation (n = 3) in parentheses. Recovery of ^{14}C in shoots, roots, and soil (% of total label applied) was 21.2%, 7.2%, 0.1% respectively in the dry season, and 25.9%, 5.8%, 0.1% in the wet season; the rest of the applied ^{14}C was respired

precipitation	depth (cm)								
(mm month^{-1})	0–1	1–5	5–10	10–15	15–20	20–30	30–40	40–50	> 50
< 200	34.9(10.1)	21.4(1.1)	10.8(4.4)	8.9(2.4)	8.1(4.2)	4.8(1.8)	4.5(0.9)	5.0(1.2)	1.7(0.2)
> 200	62.1(11.3)	14.9(4.5)	6.7(2.8)	5.1(2.8)	2.3(1.3)	3.7(1.2)	2.6(0.7)	2.0(0.9)	0.7(0.4)

Table 4. Belowground biomass (g C m^{-2}) and production (g C m^{-2} yr^{-1}) for forest and pasture at the Hapludand site. Total root biomass of the forest (including roots in litter layer and $>$ 60 cm depth) and its distribution with depth in three diameter classes ($<$ 2 mm, 2–10 mm, $>$ 10 mm) are from Raich (1980). For the pasture sites root biomass, annual root production and root distribution with depth are results of the $^{14}CO_2$ pulse labelling experiment, averaged for determinations over wet and dry seasons, and scaled to aboveground biomass as observed in the field. The residence time (RT) of pasture roots at different depth was calculated as the ratio of root biomass and annual root production

	forest biomass of roots			pasture roots *Axonopus compressus*		
	fine	medium	coarse	biomass	production	RT(yr)
total:	320	450	680	332	246	1.30
depth(cm)						
0–5	131.4	167.3	609.1	161.7	149.6	1.08
5–10	25.4	52.9	7.0	41.4	41.7	0.99
10–15	11.2	18.5	1.5	30.8	15.1	2.04
15–20	8.1	18.5	0.4	23.9	11.0	2.17
20–25	7.6	13.9	0.3	18.8	8.0	2.35
25–30	6.8	12.5	0.2	14.7	6.0	2.44
30–35	6.0	11.1	0.1	11.5	4.5	2.57
35–40	5.2	9.7	0.1	9.0	3.3	2.70
40–45	4.4	8.3	0.0	7.0	2.5	2.85
45–50	3.6	6.9	0.0	5.5	1.8	2.98
50–55	3.4	6.5	0.0	4.3	1.4	3.20
55–60	3.3	6.1	0.0	3.4	1.0	3.33

studies (Volkoff & Cerri 1987; Desjardins et al. 1991; Balesdent et al. 1993; Veldkamp 1994).

Respiration of SOC and added glucose

In the incubation experiment respiration rates, expressed as CO_2 production per amount of SOC were higher by a factor of 3–5 for surface soil samples than for samples from below 20 cm depth (Figure 2).

Respiration of glucose was more than 5 times faster in surface soils than in subsoils (Figure 3). In subsoil samples glucose respiration appeared to be limited by nutrient availability: rates increased significantly after addition of the nutrient solution, but still remained much slower than in surface soil samples.

Table 5. Bulk densities (g cm^{-3}) of Humitropept and Hapludand soils from forest and pasture sites

	Andic Humitropept					Eutric Hapludand	
depth	forest	pasture				forest	pasture
(cm)	1992	3 yr	5 yr	10 yr	18 yr	1992	25 yr
0–5	0.66	0.83	0.81	0.84	0.97	0.58	0.82
5–10	0.67	0.83	0.79	0.84	0.97	0.63	0.85
10–15	0.68	0.78	0.79	0.84	0.98	0.68	0.88
15–20	0.74	0.77	0.75	0.84	0.92	0.73	0.88
20–25	0.73	0.77	0.73	0.80	0.87	0.76	0.89
25–30	0.73	0.77	0.72	0.78	0.87	0.80	0.91
30–35	n.d.	n.d.	n.d.	n.d.	n.d.	0.83	0.92
35–40	0.72	0.79	0.73	0.77	0.87	0.80	0.91
55–60	0.74	0.82	0.77	0.80	0.85	0.85	1.00
85–90	0.79	0.83	0.79	0.81	0.87	1.01	1.07

Modelling results

Residuals between observed and simulated state variables were much larger for constant than for variable decomposition rates with depth, especially for SOC and δ^{14}C (Table 7). In fact, the model with constant decomposition rates with depth fitted the data so badly, that henceforth we only considered variable k's with depth. The diffusion coefficient D had a distinct optimum value, which was much smaller for the Humitropept (0.42 cm^2 yr^{-1}) than for the Hapludand (3.97 cm^2 yr^{-1}) chronosequence (Figure 4). Optimized decomposition rates decreased with depth. The decrease became less when increasing D from zero to its optimum (Figure 5), but it was still very strong at the optimum D value (Figure 6). In conclusion, the calibration of the model clearly showed that both diffusional transport and depth-dependent decomposition rates were necessary for proper simulation of the data. The trend of slower simulated decomposition rates at greater soil depth resembled the trend observed in the incubation experiment (Figure 2).

The optimum values for the turnover rates (k_a, k_s and k_p), for transfer between SOC pools (ϵ_a and ϵ_s), as well as the isotope fractionation factor α are given in Table 7. In an initial analysis, optimum values for k_a were 0.26 yr^{-1} for the Humitropept and 1.23 yr^{-1} for the Hapludand. However, the model appeared very insensitive to k_a, which therefore was fixed at a value of 1 yr^{-1} (in doing so, RSS increased by only 4.5% and 1.2% respectively if optimizing the other parameters again). The residence time ($1/k_s$) of the slow SOC pool was distinctly lower for the Humitropept (90 yr) than for the Hapludand (146 yr). The passive SOC pool had a residence time of several thousands of years.

Table 6. Soil organic carbon (g m^{-2} per 5cm depth), $\delta^{13}C$ and $\delta^{14}C$ of forest-pasture chronosequences of Humitropept and Hapludand soils

Andic Humitropept												
	SOC					$\delta^{13}C$					$\delta^{14}C$	
depth	forest	pasture				forest	pasture				forest	pasture
(cm)	1992	3 yr	5 yr	10 yr	18 yr	1992	3 yr	5 yr	10 yr	18 yr	1994	18 + 2yr
0– 5	1587	2100	1701	1747	1746	–27.01	–23.58	–22.85	–18.86	–19.75	175	162
5–10	1099	863	1248	928	1314	–26.45	–26.06	–25.96	–23.21	–20.94	n.d.	n.d.
10–15	826	663	739	592	990	–26.31	–26.08	–25.53	–23.68	–22.93	19	–41
15–20	629	508	521	400	657	–26.17	–25.74	–25.26	–23.27	–23.09	n.d.	n.d.
20–25	551	450	380	392	637	–24.94	–25.41	–25.09	–23.61	–23.75	n.d.	n.d.
25–30	464	404	349	332	515	–24.65	–25.60	–25.00	–22.76	–23.87	–101	–192
35–40	356	352	256	308	444	–24.36	–25.46	–24.48	–23.47	–23.79	n.d.	n.d.
55–60	263	250	227	284	323	–24.25	–24.41	–24.28	–23.77	–23.16	–281	–287

Table 6. Continued

	Eutric Hapludand					
	SOC		δ^{13}C		δ^{14}C	
depth (cm)	forest 1992	pasture 1992	forest 25 yr	pasture 25 yr	forest 1994	pasture 25 + 2 yr
0–5	2146	1620	–27.22	–21.70	163	148
5–10	2659	1815	–27.59	–21.60	n.d.	n.d.
10–15	1584	1421	–26.54	–22.88	90	77
15–20	1099	1228	–25.98	–24.80	n.d.	n.d.
20–25	1391	1153	–25.79	–25.10	n.d.	n.d.
25–30	852	978	–25.71	–25.12	–39	–22
30–35	639	998	–25.37	–24.79	n.d.	n.d.
35–40	628	828	–25.51	–24.84	n.d.	n.d.
55–60	612	490	–25.08	–24.79	–75	–83

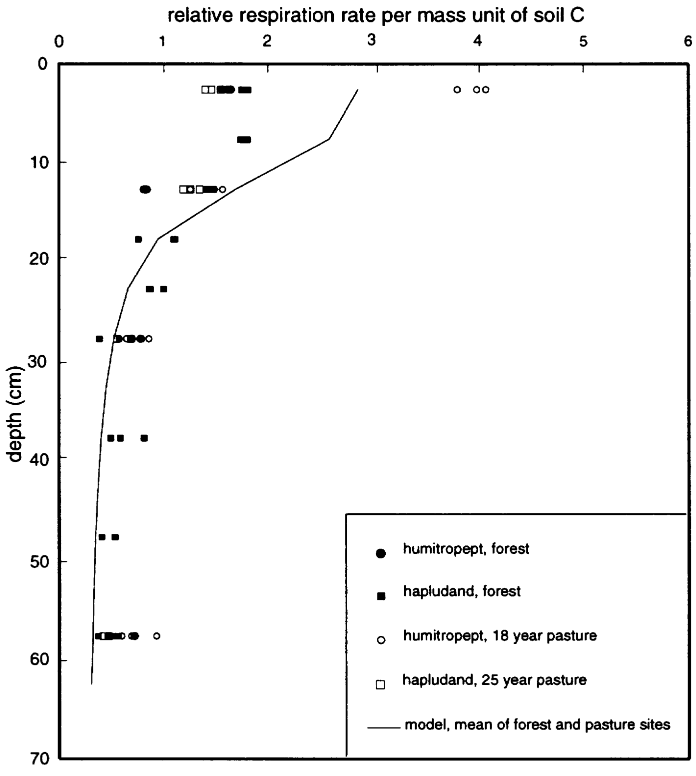

Figure 2. Respiration rates per amount of soil C at different soil depths for Humitropept and Hapludand forest and pasture soil. Respiration rates were standardized to 1 for the forest soil samples from 15–20cm depth. Forest had been replaced by pasture 18 and 25 years ago at the Hapludand and Humitropept sites respectively.

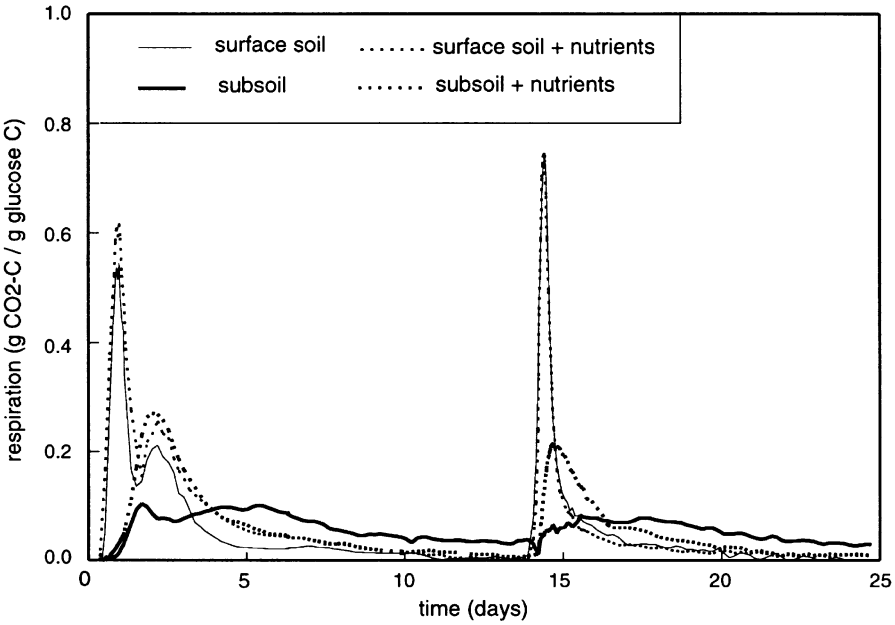

Figure 3. Respiration of glucose in an incubation experiment with Hapludand forest soil surface soil (0–5 cm depth) and subsoil (55–60 cm depth). The samples were incubated with or without addition of nutrients to the added glucose solution.

For both soils, the calibrated value of the isotope discrimination factor was close to 3‰, in agreement with isotope fractionation during soil respiration reported by Bertram (1986), and measured isotope fractionation (3.4‰) in respiration of glucose by *Escherischia coli* (Blair et al. 1985).

The sensitivity analysis (Table 8) revealed that k_p was a more sensitive parameter in the Hapludand than in the Humitropept chronosequence. The product of ϵ_s and k_p could be identified with a higher sensitivity than parameter k_p itself. This means that either a smaller c.q. larger amount of slow C transferred to passive C with lower c.q. higher turnover rate, could be identified better than the turnover rate k_p by itself. In particular for the Humitropept chronosequence – with pastures of 4 different ages – the isotope discrimination factor α was a highly sensitive parameter, especially with respect to the ^{13}C data. Most of the parameters describing the decomposition rates with depth (p_{2f} - p_{4f} and p_{1p} - p_{4p}) were very sensitive to the SOC data; the sensitivity of these parameters to the isotope data was highest in the Hapludand. Judged by Table 8 the model seems to be rather insensitive to the value of the diffusion coefficient D. However, in our sensitivity analysis parameters were varied by 5% only, and for a wider range of variation an optimum value of D could be clearly identified (Figure 4).

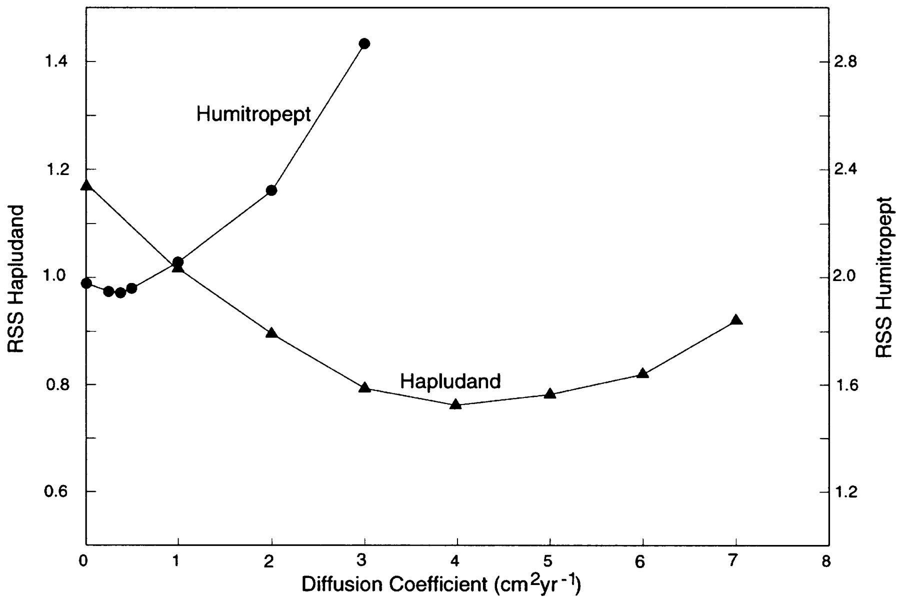

Figure 4. Total sum of squared residuals for the Hapludand and Humitropept chronosequences at different values of the diffusion coefficient D. For each value of D all parameters indicated in Table 8 were optimized again.

Table 7. Calibrated values of model parameters for the Humitropept and Hapludand forest-pasture chronosequences. First order rate constants k_a, k_s and k_p apply for the 15–20cm depth interval; compare Figure 4 for relative rates at different depths in forest and pasture soils. Sum of squared residuals (RSS) is indicated for SOC, δ^{13}C and δ^{14}C separately. Residuals indicated in italics apply for model calibration without depth-dependent decomposition

parameter	$1/k_a$	$1/k_s$	$1/k_p$	ϵ_a	ϵ_s	α	D	SSR			
units	yr	yr	yr	%	%	‰	cm^2 yr^{-1}	SOC	δ^{13}C	δ^{14}C	total
Humitropept	1.0*	92	7022	37.2	1.75	3.20	0.42	0.75$	1.09$	0.18	2.01
								1.07	*1.93*	*2.32*	*5.32*
Hapludand	1.0*	146	4588	33.3	5.32	2.78	3.97	0.28	0.21	0.26	0.76
								1.26	*0.46*	*0.55*	*2.27*

* k_a was fixed at a value of 1 yr^{-1}.

$ number of data points was 40 for the Humitropept and 18 for the Hapludand, and this results in higher residuals for the Humitropept.

Comparing observed and simulated values of carbon contents and isotope data (Figure 7) shows that the simulation model was least successful for some SOC and δ^{13}C observations in surface soils ($<$ 15 cm). For the δ^{13}C

Table 8. Sensitivity of parameters (Kolmogorov-Smirnov d-statistic) obtained by varying parameter values according to a uniform distribution around their optimum value by –2.5 to +2.5%. Parameters p_{2f} through p_{4f} describe the depth-dependent decomposition rate for the forest soils, and p_{1p} through p_{4p} the rate for the pasture soils (cf. Equation (2); given parameter values are valid if depth is measured in dm below the top of the litter layer)

		Humitropept					Hapludand				
par.	unit	optimum	sensitivity to				optimum	sensitivity to			
name		value	SOC	δ^{13}C	δ^{14}C	all 3	value	SOC	δ^{13}C	δ^{14}C	all 3
k_s	yr^{-1}	0.0109	0.102	0.053	0.243	0.064	0.0068	0.245	0.220	0.215	0.052
k_p	yr^{-1}	0.00014	0.215	0.024	0.181	0.107	0.00022	0.041	0.057	0.056	0.079
ϵ_a	–	0.0372	0.180	0.068	0.118	0.107	0.0333	0.216	0.076	0.107	0.152
ϵ_s	–	0.0175	0.220	0.044	0.066	0.149	0.0532	0.043	0.053	0.037	0.082
$\epsilon_s \cdot k_p$	yr^{-1}		0.319	0.063	0.181	0.218		0.029	0.062	0.067	0.096
α	–	0.0032	0.054	0.314	0.062	0.222	0.0028	0.049	0.069	0.047	0.102
D	$cm^{-2}yr^{-1}$	0.4200	0.067	0.042	0.069	0.051	3.9700	0.028	0.028	0.061	0.043
p_{2f}		0.1184	0.286	0.114	0.075	0.182	0.4315	0.172	0.332	0.318	0.155
p_{3f}		3.2206	0.325	0.157	0.042	0.154	9.9778	0.147	0.134	0.158	0.057
p_{4f}		0.8423	0.124	0.102	0.081	0.044	1.6501	0.635	0.590	0.492	0.303
p_{1p}		3.7972	0.208	0.050	0.111	0.162	2.7573	0.058	0.260	0.361	0.166
p_{2p}		0.2885	0.043	0.041	0.056	0.041	0.0650	0.139	0.243	0.313	0.086
p_{3p}		3.2542	0.019	0.022	0.048	0.033	4.6500	0.030	0.044	0.086	0.042
p_{4p}		3.3816	0.069	0.038	0.041	0.045	1.6553	0.085	0.100	0.108	0.100

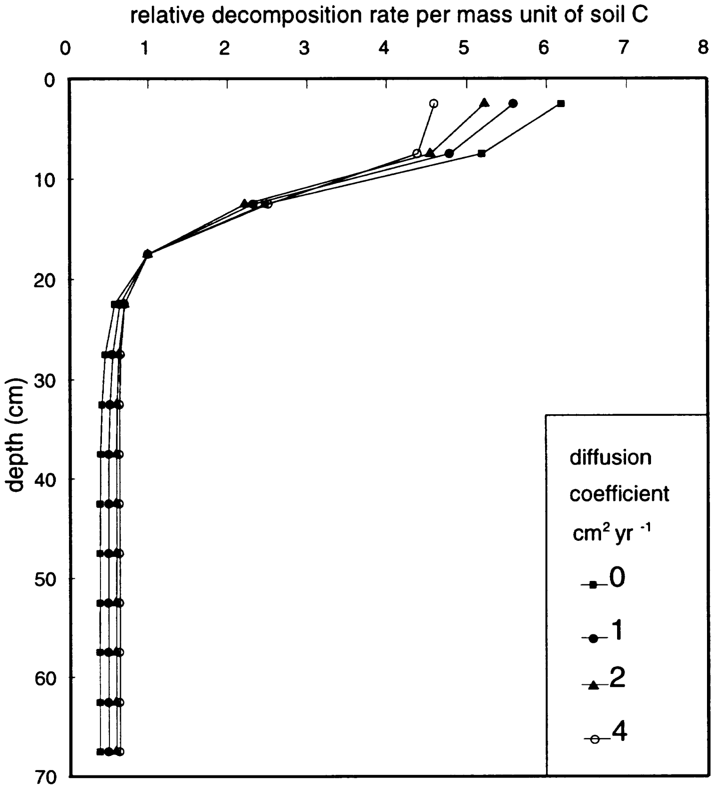

Figure 5. Relative decomposition rates of SOC at different depth in the Hapludand forest soil, as optimized for various rates of diffusion. Decomposition rates as a function of depth were parametrized according to equation (2).

data of the Humitropept chronosequence the model deviated most from a few unexpected observations; i.e. at 0–5 cm depth δ^{13}C values were higher for 3 yr than for 5 yr pasture, and also higher for 10 yr than for 18 yr pasture. However, the general trends of much larger increases of δ^{13}C values in surfaces soils than in subsoils and, especially, the relatively steep decrease with depth of δ^{14}C in the Humitropept were reproduced very well by the model.

The distribution of accepted runs over classes of parameter values for k_s, e_a, α and the product of e_s and k_p clearly shows that the addition of the isotope data to the SOC data considerably improved the identifiability of the parameters, resulting in more steeply constrained distributions (Figure 8).

Simulated annual changes of SOC in the Humitropept and Hapludand soils after conversion from forest to pasture are shown in Figure 9. The litter layer was excluded in these calculations, because of its irregular redistribution during clearing and piles of branches left at the sites. The largest decrease in

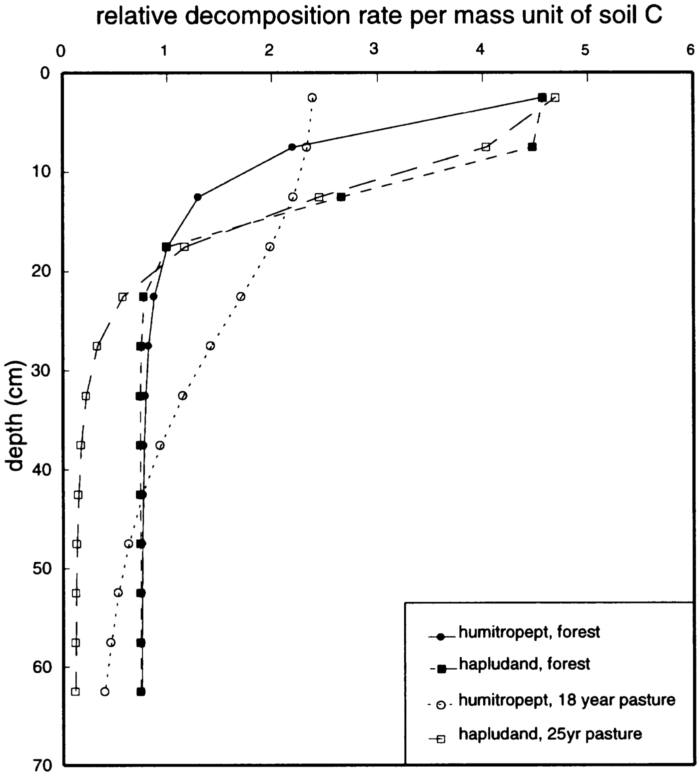

Figure 6. Relative decomposition rates of SOC at different depth in Humitropept and Hapludand forest and pasture soils. The curves apply for calibrated diffusion coefficients of 0.38 cm^2 yr^{-1} for the Humitropept and 3.97 cm^2 yr^{-1} for the Hapludand soils.

SOC occurred in the first year of pasture establishment. Thereafter SOC in the Humitropept hardly decreased, but in the Hapludand the decline of SOC to a depth of 0.65 m was between 130 and 70 g m^{-2} yr^{-1}, resulting in a simulated loss of 2590 g m^{-2} ha^{-1} between 1967 and 1992. During this period the observed loss of SOC in the Hapludand was 2180 g C m^{-2}, if changes in bulk density are taken into account. In the Humitropept the observed loss between 1974 and 1992 was 150 g C m^{-2}.

Discussion

Pulse labelling was done on undisturbed soil columns surrounded by tubes which may have influenced the results compared to a field situation. If root biomass is used as an indicator for amount of disturbance, the tubes had a minor influence on the total root biomass (752 g C m^{-2} for the field, compared

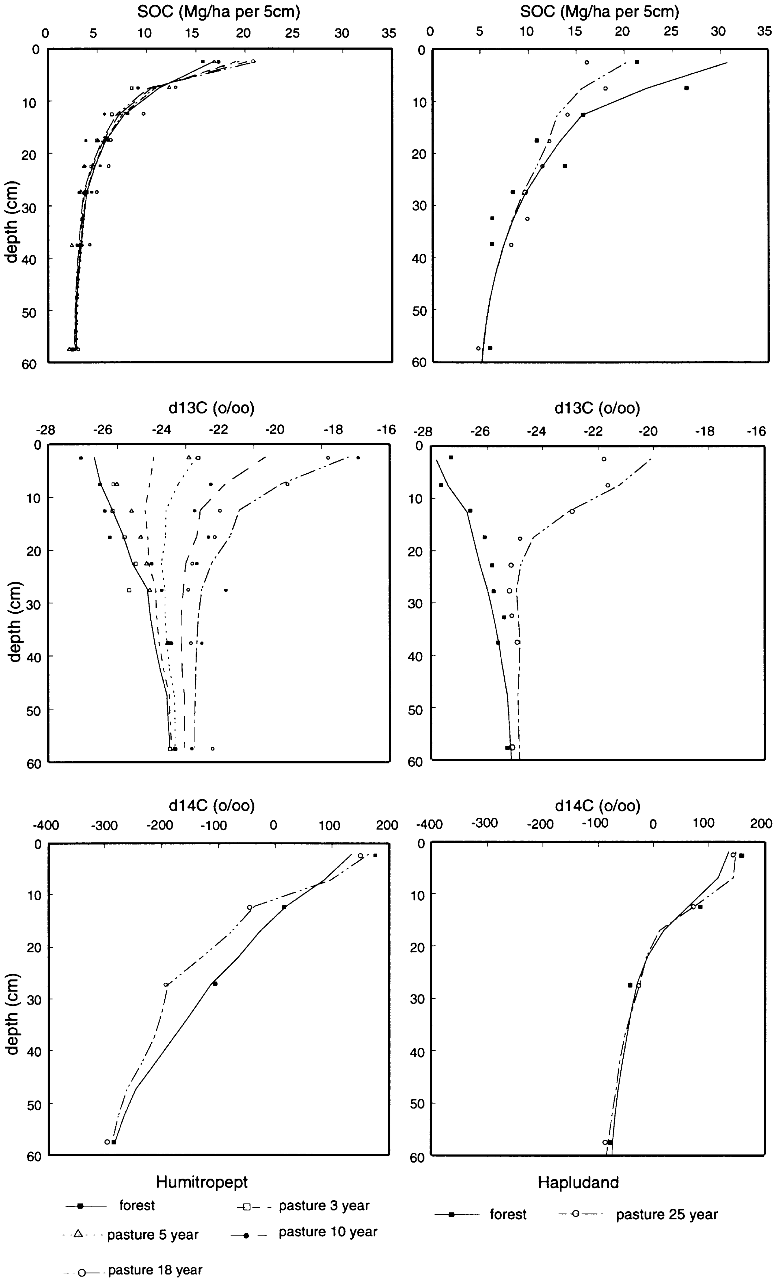

Figure 7. Observed and simulated values of SOC, δ^{13}C and δ^{14}C for steady state forest and after 18 years (Humitropept) or 25 years (Hapludand) of pasture.

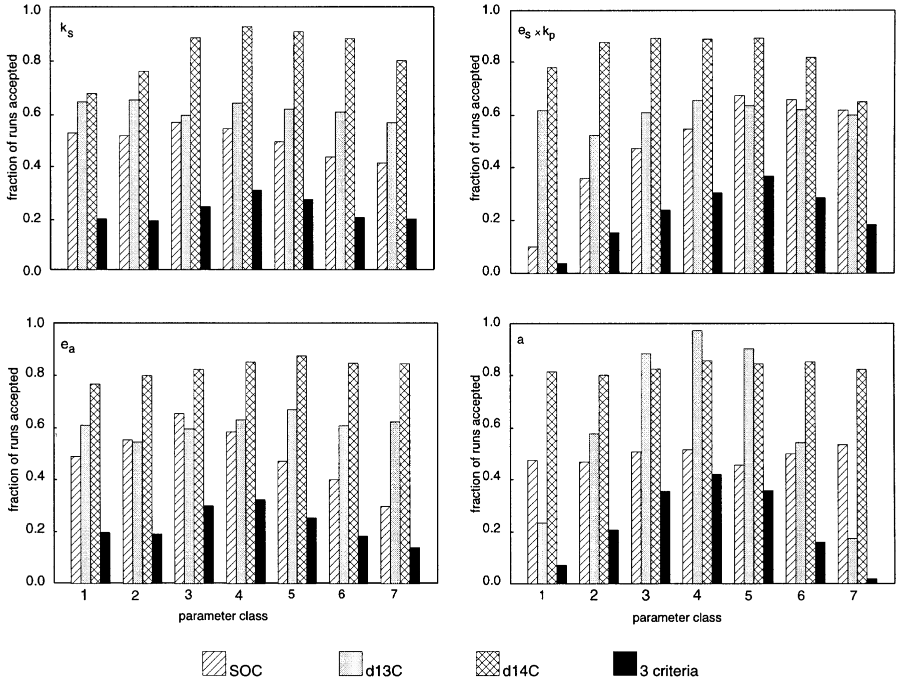

Figure 8. Fraction of accepted runs, out of a total of 2000, for which parameters were randomly varied according to a uniform distribution by –2.5 to +2.5% around their optimum value. Parameter values were divided in 7 equidistant classes and runs were accepted if residuals for SOC, δ^{13}C and δ^{14}C were less than the minimum + 2 times the standard deviation of residuals for all 2000 runs. Distributions shown are for parameters k_s, e_a, α and the product of e_s and k_p (cf. model description section for connotation of parameters).

to 778 g C m^{-2} for the tubes), but they did affect the distribution with depth; in the field a lower fraction of total C in roots was found below 40 cm depth than in the tubes (0.005 vs. 0.037), but a higher fraction between 10 and 40 cm depth (0.347 vs. 0.242). Moreover, the shoot dry matter production as extrapolated from measured production in the tubes to m^{-2} was higher than the production measured by CATIE (1989) in field plots. CATIE collected data on the same soil type at the same experimental station with the same cutting procedure. The higher production in the tubes might be due to lack of competition for space outside the tubes, and the soil cover inside the tubes was close to 90%, whereas the ground cover in the pasture is typically about 40% (Ibrahim, pers. comm.).

In ^{14}C-pulse labelling experiments several assumptions need to be satisfied for proper calculation of root turnover. Specific activity should be equal in all newly growing plant parts, and allocation of photosynthate formed during labelling should be complete at the time of harvesting. For more

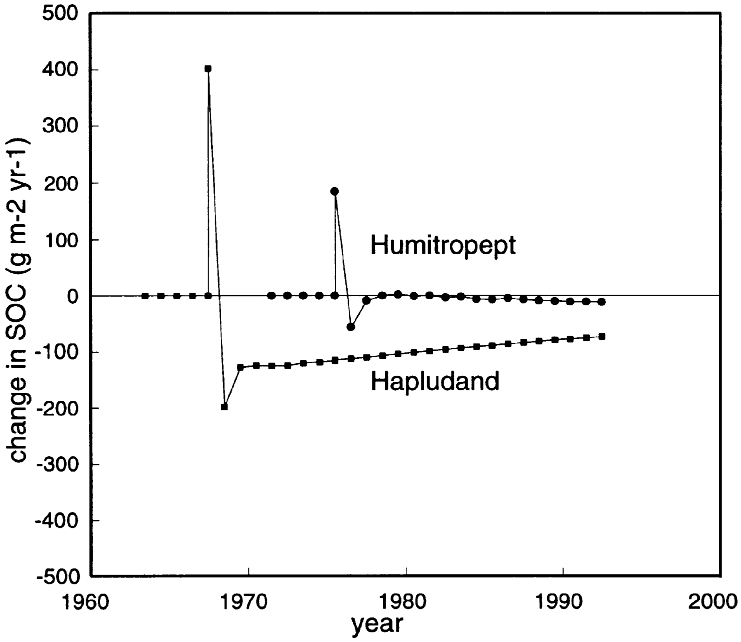

Figure 9. Annual changes in SOC stocks (0-65 cm soil depth) as simulated for soils at which native tropical forest had been replaced by grazed pastures 18 (Humitropept) and 25 (Hapludand) years ago. The slight increase of SOC immediately after forest clearing occurs through extra input during clearing (10% of leaves were assumed to be left on the soil during clearing).

elaborate discussions on these assumptions reference is made to Veldkamp (1993) and Milchunas and Lauenroth (1992). We only measured C-input with depth for the Hapludand, but could also make an estimate of the C-input for the Humitropept. In our pulse labelling experiment determination of the distribution of ^{14}C between shoots and roots and ^{14}C allocation to roots at different depths was the main objective. We assumed that the relation between aboveground production and the ratio of allocation of C to shoots and roots was equal at both soil types, but the measured aboveground production on the Humitropept was much lower, in line with a lower fertility of this soil than of the Hapludand (Table 1).

Of the C isotopes, we will only discuss the δ^{14}C data, because the data on TOC and δ^{13}C data were discussed earlier (Veldkamp 1994). The incorporation in the soil organic matter of ^{14}C produced by thermonuclear bomb testing is an indicator of SOM turnover rates on decadal and shorter time scales (Trumbore et al. 1995). The high positive δ^{14}C values for all sites point to rapid turnover rates for most of the organic matter in the top soil. The faster decrease with depth of δ^{14}C values in the Humitropept compared to

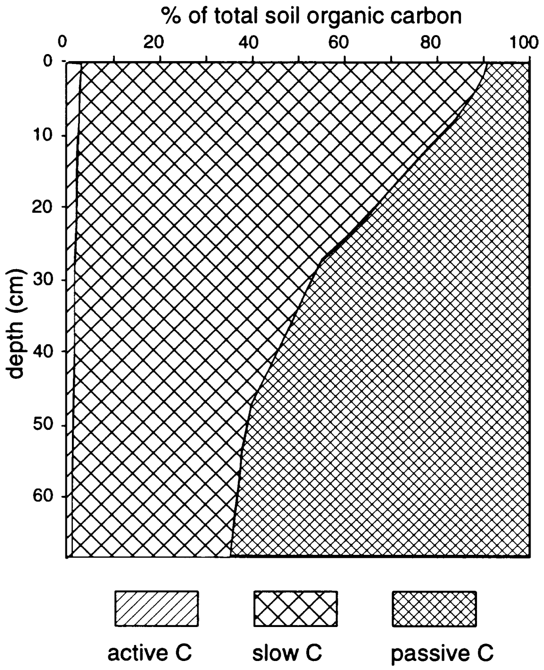

Figure 10. Contributions of 'active', 'slow' and 'passive' soil organic carbon pools to total SOC for steady state Humitropept forest soil as a function of depth.

the Hapludand, indicates that at depth, SOC turnover in the Humitropept is slower than in the Hapludand. Higher δ^{14}C values in almost all forest samples, indicate that the pastures are losing carbon on all depths compared to the original forest. Compared to an Oxisol sampled by Trumbore et al. (1995) in Brazil, our δ^{14}C numbers for the forest topsoil look very similar, but in the pasture our δ^{14}C numbers tend to be higher, which probably indicates a higher productivity of the Humitropept pasture, compared to the Brasilian pastures (which were degraded). Contrary to the Hapludand, the δ^{14}C numbers of the Humitropept follow more or less the same pattern with depth as the Brazilian Oxisol. We did not sample for ^{14}C below 60 cm, so we cannot compare the deep SOC dynamics with the situation in Brazil.

As a result of our modelling approach, we could made estimates of the diffusion coefficient D and the decline of decomposition rates with depth. The diffusion coefficient in the Humitropept was ten times smaller than in the Hapludand. This agrees with a stronger faunal turbation in the Hapludand compared to the Humitropept, presumably by species of leafcutter ants such as *Atta cephalotes* (Alvarado et al. 1981). The Hapludand pasture soil also had abundant burrows of earthworms (*Pontolex corethrurus*), that penetrated to a depth of 40 cm, but were absent in the Humitropept pasture soils. The two soils differ greatly in general fertility, with the younger Hapludand having higher contents of base cations than the older, more weathered Humitropept. The relatively constant decomposition rates in the Hapludand in the upper 15 cm, against steeply declining k values in the Humitropept are in accordance with a thicker dark A-horizon in the Hapludand (0–25 cm), compared to the Humitropept (0–15 cm). The structure of the Hapludand A-horizon is also more strongly biogenic than that of the Humitropept.

The observed decreasing respiration rates with soil depth can be due to (i) smaller contributions to total SOC of carbon pools with fast turnover (C_a and/or C_s) at greater depth (cf. Figure 10), (ii) slower decomposition of individual SOC pools at greater depth. The latter effect was observed for added glucose, which was respired more than 5 times faster in surface soils than in subsoils. The calibrated depth-dependent decomposition rates compare favourably with measured relative respiration rates per amount of soil C (Figure 2). However, in this respect it should be realized that for ‘active C’ and ‘slow C’ the contribution to total SOC decreases with depth, whereas that of ‘passive C’ increases (Figure 10). Tracing the origin of CO_2 from the 3 pools of SOC distinguished by determining ^{14}C in respired CO_2 might have contributed to further constrain our model, but we did no such determinations. We also determined ^{14}C in bulk SOC only, and no physical and chemical fractionation methods were employed, which might have allowed for a comparison between calibrated and experimentally determined SOC pools with different residence time, and thus with different ^{14}C content (Trumbore et al. 1995).

The slower respiration of added glucose at deeper samples in our incubation study revealed that the decreasing decomposition rates could not be explained solely by a smaller contribution of easily decomposable SOC pools at greater depth. Limited oxygen supply may play a role in the field situation, but probably not in our incubation studies, because the samples were first air dried and then brought to an equal moisture content. Nutrient limitation is one of the factors, as was demonstrated by the increase in respiration after addition of nutrients, but even then respiration of glucose was still slower in subsoil than in surface soil samples. A factor left might be slower diffusion of substrate to microbial populations, caused by differences in soil structure and specific surface area.

Although the decline of decomposition rates with depth became less pronounced when D increased from zero to the optimum value (Figure 5), we could not satisfactory model the observed SOC and isotope values by only considering a diffusion coefficient and without considering declining decomposition rates. This contrasts with results of Elzein and Balesdent (1995), who found that at constant decomposition rates with depth, diffusion and vertical mass transport could explain SOC stocks and ^{14}C contents. We have demonstrated that diffusion of SOC and declining decomposition rates with depth are important features that work in parallel and should both be considered when SOC dynamics in deeper layers is studied. However, this can only be done when vegetation productivity is measured instead of modelled and is combined with inventories of SOC and ^{13}C and ^{14}C measurements. The present study is unique in that we measured the C-input as a function of depth by pulse labelling with $^{14}CO_2$. Knowing the C-input gives the opportunity to calculate turnover rates of SOC fractions. In other modelling studies (O'Brien & Stout 1978; O'Brien 1984; Jenkinson et al. 1992; Jenkinson & Coleman 1994; Elzein & Balesdent, 1995) the C-input is normally calibrated given the estimated turnover rates of SOC fractions. In this study the C-input with depth was most accurately measured for the Hapludand, because our pulse labelling experiment was conducted at this site. At the Humitropept site production, aboveground biomass and root biomass with depth were measured too, but estimates of belowground input are less certain, because they are based on regression analysis of aboveground production and carbon allocation to shoots vs. roots of the ^{14}C-pulse labelling experiment on the Hapludand.

We could evaluate SOC turnover rates at different depths and evaluate which processes may influence the depth distribution of SOC and naturally occurring δ^{13}C and δ^{14}C after deforestation. We furthermore showed that more than 50% of the SOC below 40 cm depth had residence times of several thousands of years. In recent years more studies on SOC dynamics have included deeper layers of the soil (Trumbore et al. 1995; Elzein & Balesdent 1995). We are of the opinion that rooting patterns, SOC pools and turnover times below the topsoil clearly deserve more attention, amongst others to assess the impact of human activities and climate change on the global C budget. Our study suggests that at similar carbon allocation to roots, soils with vegetation with deeper roots will in the long term sequester more carbon than shallowly rooted soils.

Isotope fractionation in SOC decomposition has been regarded to be one of the mechanisms causing increasing δ^{13}C values with soil depth in the forest soils. An additional reason for increasing δ^{13}C with soil depth is related to the decrease in atmospheric $^{13}CO_2$ (and $^{14}CO_2$; the so-called Suess effect) due to fossil fuel burning, which has resulted in a decrease of δ^{13}C values in phytomass of approximately 1.5‰ since 1800 (Leavit & Long 1988). An increase in δ^{13}C of 2–3‰ between 0 and 1m depth has also been observed in many ferralitic soils under C-3 forest in Brazil (Desjardins et al. 1991). Our interpretation of the increase of δ^{13}C with soil depth involves isotopic fractionation during SOC decomposition, as well as the effect of transport of

SOC fractions; during net downward transport a large part of SOC fractions with fast decomposition rates will be respired, giving rise to a relative increase of SOC fractions with slower turnover and higher δ^{13}C values at greater depth. Also the decreasing δ^{14}C values with soil depth are caused by such a chromatographic effect; a large part of recent C input at the soil surface will be lost during transport, before being stabilized in SOC fractions with slower turnover at greater depth. The decrease of δ^{14}C with soil depth is steeper in the Humitropept than in the Hapludand, reflecting the slower dispersion in the Humitropept.

Not all data were equally important for the calibration of different parameters of our model. The k_a, k_p, and ϵ_a parameters were very sensitive to the C inventory data while k_s and k_p were strongly influenced by the ^{14}C data, which confirms the findings by Trumbore et al. (1995) that ^{14}C is a more sensitive indicator of changes in carbon stocks over the past 30 years than inventory measurements. Our data set was not suitable to accurately determine the decomposition rate (k_a) of the ‘active’ SOC fraction. This is not surprising, considering that 3 and 25 years after forest clearing had elapsed before the pasture sites were sampled. The isotope fractionation factor α appeared to be mainly defined by the ^{13}C data. Total SOC appeared to be of paramount importance to determine optimal values for parameters k_a, k_p, ϵ_a and the product $\epsilon_s \cdot k_p$. The ^{14}C data contributed most to delimit parameter values for k_s and k_p, and to a lesser extent to constrain ϵ_a and $\epsilon_s \cdot k_p$. By including the ^{14}C data, the 1-st order decomposition rate k_s was most clearly delimited at low parameter values and k_p at high parameter values. The distribution of the isotope fractionation factor α was determined mainly by the ^{13}C data.

Parameter ϵ_a in our model might be compared with microbial carbon-use-efficiency of plant litter. C-use efficiency is commonly between 0.3 and 0.6, mainly depending on the concentration of lignin. Easily degradable substrates, such as glucose and starch, are frequently used with a high efficiency, but also the subsequent turnover of microbial necromass determines which fraction of originally consumed C is eventually stabilized into humus compounds (Baldock et al. 1989).

Differentiation of plant litter with respect to its chemical composition (content of lignin, (hemi)cellulose, proteins etc.), each with a specific δ^{13}C value, is not included in our model. During decomposition of litter, δ^{13}C may initially decrease due to differential preservation of lignin which is low in ^{13}C (Ågren et al. 1996), but in later stages of decomposition this effect is largely counteracted or usually even reversed by isotope discrimination against ^{13}C during soil respiration (Wedin et al. 1995). Therefore effects of differential preservation of lignin on δ^{13}C of remaining soil organic matter are thought to be significant only in short term ($<$ 2 yr) decomposition studies.

Knowledge on turnover times of SOC fractions is crucial in model predictions of net emission or sequestration of C in ecosystems. The calibration of our model showed that residence times of SOC increased with soil depth, and that a large fraction had a residence time of several thousands of years. At a time-scale of decades or a few centuries this stable C will only marginally contribute to changes in SOC stocks. On the other hand, several decades to a few centuries are still considered ‘ages’ in most SOC research, and few long-term studies of SOC dynamics are available to improve our mechanistic understanding of SOC cycling at this time-scale, which is of major interest from the perspective of global change.

Conclusions

- Soil organic carbon dynamics in a Hapludand and a Humitropept soil were simulated for forest-pasture chronosequences, in which the change of lowland tropical rainforest (C3-vegetation) to low productive pastures (C4-vegetation) resulted in large changes in δ^{13}C.
- For steady state forest soils, δ^{13}C increased with depth, due to isotopic discrimination of ^{13}C against ^{12}C during soil respiration; the isotope discrimination factor was 3‰.
- For the Humitropept soil SOC stocks stayed more or less constant after deforestation, but they decreased by 2200 g m^{-2} in the Hapludand after 25 years of pasture.
- Calibration of the model with three pools of soil organic carbon (‘active’ C, ‘slow’ C and ‘passive’ C) to data on SOC, δ^{13}C and d^{14}C revealed that slow C contributed most to SOC stocks in surface soils, and that passive C contributed most below 40 cm depth.
- The decomposition rate of active C was an insensitive parameter, that could not properly be identified from our dataset; residence time of slow C was 90 yr in the Humitropept and 146 yr in the Hapludand, whereas the residence time of passive C was several thousands of years (all values only valid in the 15–20 cm layer of the soils).
- Decomposition rates of soil organic carbon fractions decreased strongly with depth; they were ± 3 times faster in surface soils (0–5 cm) than below 40 cm depth.
- Vertical transport of C by biotic and physical mixing processes could be simulated as a diffusion process, with a diffusion constant of 0.42 cm^2 yr^{-1} in the Humitropept and 3.97 cm^2 yr^{-1} in the more fertile Hapludand, in agreement with showing a higher rate of bioturbation according to soil profile morphology.

Acknowledgements

This Study was supported by the Netherlands Foundation for the Advancement of Tropical Research (WOTRO). We thank A.G. Jongmans for investigating soil profile morphology.

References

Ågren GI Bosatta E & Balesdent J (1996) Isotope discrimination during decomposition of organic matter: A theoretical analysis. Soil Sci. Soc. Amer. Proc. 60: 1121–1126

Alvarado A, Berish CW & Peralta F (1981) Leaf-cutter ant (Atta cephalotes) influence on the morphology of andepts in Costa Rica. Soil Sci. Soc. Amer. Proc. 45: 790–794

Amato M (1983) Determination of carbon ^{12}C and ^{14}C in plant and soil. Soil Biol. & Biochem. 15: 611–612

Baldock JA, Oades JM, Vasallo M & Wilson MA (1989) Incorporation of uniformly labelled ^{13}C-glucose carbon into the organic fraction of a soil. ^{13}C nmR measurements. Soil Biol. & Biochem. 27: 725–746

Balesdent J, Wagner GH & Mariotti A (1988) Soil organic matter turnover in long-term field experiments as revealed by the carbon-13 natural abundance. Soil Sci. Soc. Amer. J. 52: 118–124

Balesdent J, Girardin C & Mariotti A (1993) Site-related δ^{13}C of tree leaves and soil organic matter in a temperate forest. Ecology 74: 1713–1721

Bertram HG (1986) Zur Rolle des Bodens im globalem Kohlenstoffzyklus. Veröffentl. Naturforsch. Gesellsch. Emben 1814, Band 8, Serie 3-D3, Osnabrück, 144 pp

Blair N, Leu A, Muños, Olsen J, Kwong E & Des Marais D (1985) Carbon isotope fractionation in heterotrophic microbial metabolism. Appl. Environ. Microbiol. 50: 996–1001

Bouwman AF (1990) Exchange of greenhouse gases between terrestrial ecosystems and the atmosphere. In: Bouwman AF (Ed) Soils and the greenhouse effect, John Wiley & Sons, Chichester, pp 61–127, 575 pp

Caceci MS & Cacheris WP (1984) Fitting curves to data. Byte: 340–362

CATIE (Centro Agronomico Tropical de Investigacion y Enseñaza) (1989) Sistemas silvopastoriles para el trópico húmedo bajo. Informe primera fase. MAG-IDA-CATIE/CIID, CATIE, Turrialba, Costa Rica. 50 pp

Desjardins T, Andreux F, Volkoff B & Cerri CC (1991) Distribution de l'isotope ^{13}C dans les sols ferralitiques du Brésil. Cahiers ORSTOM, Série Pédologie, 26(4): 343–348

Desjardins T, Andreux F, Volkoff B & Cerri CC (1994) Organic carbon and ^{13}C contents in soils and soil size-fractions, and their changes due to deforestation and pasture installation in eastern Amazonia. Geoderma 61: 103–118

Detwiler RP (1986) Land use change and the global carbon cycle: the role of tropical soils. Biogeochemistry 2: 67–93

Detwiler RP & Hall CAS (1988) Tropical forest and the global carbon cycle. Science 239: 42–47

Elzein A & Balesdent J (1995) Mechanistic simulation of vertical distribution of carbon concentrations and residence times in soils. Soil Sci. Soc. Amer. J. 59: 1328–1335

Fisher MJ, Rao IM, Ayarza MA, Lascano CE, Sanz JI, Thomas RJ & Vera RR (1994) Carbon storage by introduced deep-rooted grasses in the South American savannas. Nature 371: 236–238

Grace PR & Ladd JN (1995) SOCRATES Soil Organic Carbon Reserves And Transformations in agro-Ecosystems, User Manual v.2.00, Cooperative Research Centre for Soil and Land Management, Glen Osmond, Australia, 23 pp

Houghton RA, Skole DL & Lefkowitz DS (1991) Changes in the landscape of Latin America between 1850 and 1985. II. Net release of CO_2 to the atmosphere. Forest Ecol. Managem. 38: 173–199

Huising J (1993) Land use zones and land use patterns in the Atlantic Zone of Costa Rica. Thesis, Agricultural University, Wageningen, 222 pp

Hunt HW (1977) A simulation model for decomposition in grasslands. Ecology 58: 469–484

Ibrahim MA (1994) Compatibility, persistence and productivity of grass-legume mixtures for sustainable animal production in the Atlantic Zone of Costa Rica. Thesis, Agricultural University, Wageningen, 129 pp

Jenkinson DS (1990) The turnover of organic carbon and nitrogen in soil. Phil. Trans. Royal Soc. London B 329: 361–368

Jenkinson DS & Coleman K (1994) Calculating the annual input of organic matter to soil from measurements of total organic carbon and radiocarbon. Europ. J. Soil Sci. 45: 167–174

Jenkinson DS, Harkness DD, Vance ED, Adams DE & Harrison AF (1992) Calculating net primary production and annual input of organic matter to soil from the amount and radiocarbon content of soil organic matter. Soil Biol. & Biochem. 24: 295–308

Keller ME, Veldkamp E, Weitz AM & Reiners WA (1993) Effect of pasture age on soil trace gas emissions from a deforested area of Costa Rica. Nature 365: 244–246

Leavit SW & Long A (1988) Stable carbon isotope chronologies from trees in the southwestern United States. Global Biogeochem. Cycles 2: 189–198

Lugo AE & Brown S (1993) Management of tropical soils as sinks or sources of atmospheric carbon. Plant and Soil 149: 27–41

Meyer HAJ & van der Plicht J (1995) Comparing long-term atmospheric ^{14}C and ^{3}H records near Groningen, The Netherlands with Fruholmen, Norway and Izaña, Canary Islands ^{14}C stations. Radiocarbon 37: 39–50

Milchunas DG & Lauenroth WK (1992) Carbon dynamics and estimates of primary production by harvest, ^{14}C dilution and ^{14}C turnover. Ecology 73: 593–607

Minson DJ & McDonald CK (1987) Estimating forage intake from the growth of beef cattle. Tropic. Grassl. 21: 116–122

Mook WG & Streurman HJ (1983) Physical and chemical aspects of radiocarbon dating. In: Mook WG & Waterbolk HTj (Eds) Proc. Groningen Symp. ^{14}C and Archeology, PACT Publ. 8: 31–55

Nadelhoffer KJ & Fry B (1988) Controls on natural nitrogen-15 and carbon-13 abundances in forest soil organic matter. Soil Sci. Soc. Amer. J. 52: 1633–1640

Nakane K (1978a) A Mathematical model of the behaviour and vertical distribution of organic carbon in forest soils. Japan. J. Ecol. 28: 111–122

Nakane K (1978b) A Mathematical model of the behaviour and vertical distribution of organic carbon in forest soils. II. A revised model taking the supply of root litter into consideration. Jap. J. Ecol. 28: 169–177

Nelder JA & Mead R (1965) A Simplex Method for Function Minimization. Computer J. 7: 308–313

Nordgren A (1988) Apparatus for the continuous, long-term monitoring of soil respiration in large numbers of samples. Soil Biol. & Biochem. 20: 955–957

Nydal R & Lovseth K (1983) Tracing bomb ^{14}C in the atmosphere 1962–1980. J. Geophys. Res. 88: 3621–3642

O'Brien BJ (1984) Soil organic carbon fluxes and turnover rates estimated from radiocarbon enrichments. Soil Biol. & Biochem. 16: 115–129

O'Brien BJ & Stout JD (1978) Movement and turnover of soil organic matter as indicated from carbon isotope measurements. Soil Biol. & Biochem. 10: 309–317

Parton WJ, McKeown B, Kirchner V & Ojima D. (1992) Century Users Manual, Natural Ecology Laboratory, Ford Collins, Colorado 80523

Parton WJ, Stewart JWB & Cole CV (1988) Dynamics of C, N, P and S in grassland soils: a model. Biogeochem. 5: 109–131

Raich JW (1980) Fine roots regrow rapidly after forest felling. Biotropica 12: 231–232

Raich JW (1983) Effects of forest conversion on the carbon budget of a tropical soil. Biotropica 15: 177–184

Rastetter EB, Ryan MG, Shaver GR, Melillo JM, Nadelhoffer KJ, Hobbie JE & Aber JD (1991) A general biogeochemical model describing the response of the C and N cycles in terrestrial ecosystems to changes in CO_2, climate and N deposition. Tree Physiol. 9: 101–126

Schimel DS (1995) Terrestrial ecosystems and the carbon cycle. Global Change Biology 1: 77–91

Scharpenseel W-H & Becker-Heidman P (1989) Shifts in ^{14}C patterns of soil profiles due to bomb carbon, including effects of morphogenetic and turbation processes. Radiocarbon 31: 627–636

Scharpenseel W-H, Becker-Heidman P, Neue HU & Tsutsuki K (1989) Bomb-carbon, 14C-dating and 13C-measurements as tracers of organic matter dynamics as well as of morphogenetic and turbation processes. Sci. Tot. Environm. 81/82: 99–110

Skjemstad JO, Le Feuvre RP & Prebble RE (1990) Turnover of soil organic matter under pasture as determined by ^{13}C natural abundance. Austral. J. Soil Res. 28: 267–276

Sombroek WG, Nachtergaele FO & Hebel A (1993) Amounts, dynamics and sequestering of carbon in tropical and subtropical soils. Ambio 22: 417–426

Stout JD, Goh KM & Rafter TA (1981) Chemistry and turnover of naturally occurring resistant organic compounds in soil. In: Paul EA & Ladd JN (Eds) Soil biochemistry, Vol. 5. Marcel Dekker, New York, pp 19–24

Sundquist E (1993) The global carbon budget. Science 259: 234–239

Thornley JHM & Johnson IR (1990) Plant and Crop Modelling. A Mathematical Approach to Plant and Crop Physiology. Clarendon Press, Oxford

Trumbore SE, Davidson EA, Barbosa de Camargo P, Nepstad DC & Martinelli LA (1995) Belowground cycling of carbon in forest and pastures of Eastern Amazonia. Global Biogeochem. Cycles 9: 515–528

Veldkamp E, Weitz EA, Staritsky IG & Huising EJ (1992) Deforestation trends in the Atlantic Zone of Costa Rica, a Case Study. Land Degrad. Rehabilit. 3: 71–84

Veldkamp E (1994) Organic carbon turnover in three tropical soils under pasture after deforestation. Soil Sci. Soc. Amer. J. 58: 175–180

Vittorello VA, Cerri CC, Andreux F, Feller C & Victória RL (1989) Organic matter and natural carbon-13 distribution in forested and cultivated oxisols. Soil Sci. Soc. Amer. J. 53: 773–778

Volkoff B. & Cerri CC (1987) Carbon isotopic fractionation in subtropical Brazilian grassland soils. Comparison with tropical forest soils. Plant and Soil 102: 27–31

Wedin DA, Tieszen LL, Dewey B & Pastor J (1995) Carbon isotope dynamics during grass decomposition and soil organic matter formation. Ecology 76: 1383–1392